

Chapter 4. The First Wafer-fused AlGaAs-GaAs-GaN HBT

4.1. Overview

The data of Chapter 3 illustrated the importance of understanding the effect of the fusion process parameters on the electrical properties and chemical composition of the resulting fused interface. Subsequently, the study described in this chapter explored a similar systematic variation of the fusion temperature in forming the GaAs-GaN base-collector junction of the HBT. An important correlation was revealed between fusion temperature, base-collector leakage, and emitter-base degradation. Fusion temperatures as low as 500-550°C were used to produce HBTs with mechanically stable and electrically active fused interfaces. HBTs were fused over a wide range of temperatures (500-750°C). However, when fused at a mid-range temperature, HBTs demonstrated optimal characteristics. The lowest fusion

temperatures produced low common-emitter output current and low current gain, whereas the highest fusion temperatures led to excessive base-collector leakage.

4.2. Transistor Design

Figure 4.1 shows the material structure of this dissertation's first and simplest HBT. The HBT was designed to be n-AlGaAs/p-GaAs/n-GaN, rather than p-AlGaAs/n-GaAs/p-GaN, in order to avoid the use of p-GaN. Promising research with GaN-based bipolar transistors is presently limited by problems associated with the p-GaN material, such as low hole mobility and low hole concentration due to the high Mg dopant activation energy.[1-14] Additionally, n-p-n HBTs are more widely used in most integrated circuit designs, as electrons tend to be lighter and faster charge carriers than do holes.[15, 16]

AlGaAs-GaAs was chosen as the emitter-base material system, due to its high emitter injection efficiency, low base transit time, high current gain, and widely reported success in HBT applications.[17-19] In contrast to GaN growth technology, AlGaAs-GaAs growth was already well developed, producing uniform low-defect material layers, which led to reproducible electrical features such as turn-on voltage. The AlGaAs-GaAs emitter-base structure was made according to a typical design often reported in conference papers, journals, and textbooks.[17, 20-23] The typical AlGaAs-GaAs emitter-base design would have allowed for a thinner base (70-150nm), and hence a reduced base transit time and increased current gain;

however, a 150nm thickness was chosen for this initial HBT in order to preserve the effective p-type doping of the base during the fusion-induced cross-diffusion of dopants (as discussed in Section 3.4). Carbon, rather than beryllium, was chosen as the p-GaAs base dopant in order to minimize dopant diffusion during the high-temperature fusion procedure (Figure 3.5).[21, 24]

The p-GaAs base was doped heavily ($1 \times 10^{19} \text{ cm}^{-3} \text{ C}$), in order to minimize the base resistance. It was important to recognize that, with a wider-bandgap emitter than base, the high base doping did not jeopardize a high emitter injection efficiency and hence current gain. The ratio of collector current (I_C) to hole back injection current (I_{Bp}) was considered for a graded HBT: [25]

$$I_C/I_{Bp} = D_{nB}/D_{pE} * N_E/N_B * W_E/W_B * \exp[(E_{gE}-E_{gB})/(k_B T)]$$

where:

- D_{nB} = minority carrier (electron) diffusivity in the base
- D_{pE} = minority carrier (hole) diffusivity in the emitter
- N_E = emitter n-typing doping
- N_B = base p-type doping
- W_E = emitter thickness
- W_B = base thickness
- E_{gE} = energy bandgap of the emitter material
- E_{gB} = energy bandgap of the base material
- k_B = Boltzmann constant ($8.62 \times 10^{-5} \text{ eV/K}$)
- T = temperature

For a first-order analysis, $D_{nB} \sim D_{pE}$ and $W_E \sim W_B$. Thus, for an emitter-base homojunction, the transistor must have $N_E > N_B$ in order to achieve $I_C/I_{Bp} > 1$ and current gain. In contrast, for a graded emitter-base heterojunction with $E_{gE} > E_{gB}$, the HBT can have $I_C/I_{Bp} \gg 1$ (and hence high current gain), even if $N_E \ll N_B$. In this

dissertation study, because the energy bandgap of the $\text{Al}_{0.3}\text{Ga}_{0.7}\text{As}$ emitter ($E_{gE} = 1.80\text{ eV}$) was greater than the bandgap of the GaAs base ($E_{gB} = 1.42\text{ eV}$), a high I_C/I_{Bp} (and hence high current gain) was possible even with the base doping ($N_B = 1 \times 10^{19}\text{ cm}^{-3}\text{ C}$) much greater than the emitter doping ($N_E = 5 \times 10^{17}\text{ cm}^{-3}\text{ Si}$).

The n-AlGaAs emitter thickness (180nm), the Al mole fraction (0.3), and the grading of the emitter-base junction were chosen to mitigate back-injection of holes from the base to the emitter, thereby maximizing emitter injection efficiency and current gain. The emitter contact metal was placed onto an n^+ -GaAs cap layer (rather than directly onto the AlGaAs emitter) in order to decrease the contact resistance.

The primary reason for combining an AlGaAs-GaAs emitter-base with a GaN collector was to investigate the extent to which a disordered wafer-fused junction could serve as a critical device active region. Additionally GaN was chosen as the collector material, because its larger energy bandgap ($E_{g, \text{GaN}} = 3.39\text{eV}$) implied that it could withstand a higher electric field than GaAs ($E_{g, \text{GaAs}} = 1.42\text{eV}$). Compared to a p-GaAs/n-GaAs base-collector, the p-GaAs/n-GaN base-collector junction was expected to withstand a higher reverse bias, allowing the HBT to operate at higher voltages without breakdown. The collector was made of the standard UCSB uid-GaN growth template[26], with a large enough thickness ($\sim 2\text{ }\mu\text{m}$) and low enough n-type doping ($10^{16}\text{-}10^{17}\text{ cm}^{-3}\text{ Si}$) to promote a higher breakdown voltage. Chapter 6 compares the high-voltage characteristics of AlGaAs/GaAs/GaN and AlGaAs/GaAs/GaAs HBTs.

Starting materials are depicted in Figure 4.1.a. Samples were formed via wafer fusion (at 500, 550, 600, 650, 700, and 750°C for one hour) using the process described in Section 2.2. I-V test structures are shown in Figure 4.1.c.

4.3. Chemical Profiles

SIMS analysis confirmed that the doping profiles of the n-p-n emitter-base-collector were preserved during the fusion anneal. An example is shown in Figure 4.2. Figure 4.3 shows the Si, C, O, and H profiles of different samples of the same HBT structure (Figure 4.1), all formed via fusion for one hour but each fused at a different temperature (500-750°C). As observed with most fused diode samples (Chapter 3), higher SIMS signal peaks were observed at interfaces fused at lower temperatures. All these data suggested that Si, C, O, and H were present at the fused interface prior to fusion (as residual impurities remaining on the surfaces of the constituent wafers), and/or the species readily diffused from the crystal bulk to the gettering fused interface early in the bonding process. With continued thermal treatment, the high concentrations of Si, C, O, and H at the interface may have driven the redistribution of these species into the surrounding materials.

As discussed in Chapter 3, this redistribution may be detrimental to the electrical quality of both the fused interface (the base-collector junction) and the surrounding areas (most critically, the base). For example, Figure 4.3 shows large concentrations of Si, C, O, and H at the fused base-collector junction. Hydrogen is

particularly interesting. Hydrogen could have readily been incorporated into the GaN layer during MOCVD growth. However, the SIMS data of AlGaAs-GaAs-GaAs HBTs (Chapter 6) suggest that significant levels of hydrogen were present at the fused junction, even when the device materials were grown exclusively via MBE, and not MOCVD. Thus, it is likely that a significant amount of hydrogen (in some chemical form) remained on the surfaces of the adjoining wafers, prior to fusion and after the cleaning procedure described in Table 2.2. The hydrogen may have originated from the methanol used in the bonding process, as described in Table 2.2. In future work, the reduction of residual pre-fusion impurities may greatly improve HBT electrical characteristics -- especially the reduction of hydrogen, a known passivating agent of C, which is used here as the p-GaAs base dopant. In carbon-doped p-GaAs, hydrogen and carbon have been shown (via infrared absorption analysis) to bond together into complexes, passivating the electrical activity of the carbon dopant.[27] The remainder of this chapter describes the likely effect on observed electrical characteristics, of hydrogen passivation in the base.

4.4. Emitter-Base Diode Characteristics

Since the performance of the n-p-n HBT depended on the behavior of its two constituent back-to-back diodes, this study first examined the current-voltage (I-V) characteristics of the base-collector and emitter-base diodes independently (Figure 4.4). The AlGaAs-GaAs emitter-base junction was formed directly through MBE

growth, but it was important to isolate the effects of the fusion or anneal conditions on the electrical characteristics of that junction (i.e. the elevated temperature for one hour, either with or without the presence of the gettering fused interface). Figure 4.4.b. shows I-V characteristics of the as-grown emitter-base diode (prior to fusion), and of the emitter-base diodes (collector-open) in HBT structures formed via wafer fusion at 700-750°C for one hour. The data shown are a subset of I-Vs for diodes in HBTs formed via fusion at 550-750°C. All emitter-base diodes exhibited an ideality factor of 1.2-1.5, similar turn-on voltage, low reverse-bias leakage current, and similar breakdown. All emitter-base I-V characteristics were nearly identical to those of the as-grown sample, except for the emitter-base diode subjected to the highest fusion temperature of 750°C, yielding a lower current at a given forward-bias voltage. Because the diode characteristics were nearly identical (in ideality factor, turn-on voltage, reverse-bias leakage current, breakdown), it was unlikely that the emitter-base junction itself was degraded during fusion. However, given the additional series resistance observed for the sample fused at 750°C, it was likely that the base of this sample was somehow degraded by the fusion process.

It was interesting to study the emitter-base diode further. Figure 4.4.c shows the I-V data of the as-grown (unannealed) diode, as well as that of a diode annealed at 750°C for one hour. (During the anneal, samples were placed face-to-face, in order to avoid surface degradation.) The two I-Vs appeared to be identical, suggesting that the elevated temperature alone had a negligible effect on diode characteristics. However, the I-V did appear to degrade for a diode fused to GaN under those same annealing

conditions (750°C for one hour). A similar discrepancy was seen in studies of GaAs-InP wafer-fused interfaces, involving structures that were similarly fused, annealed, or as-grown; device characteristics of the as-grown material were somewhat degraded after annealing, but were degraded even further after wafer fusion at the same temperature (i.e. annealed in the presence of a nearby fused interface).[28] Thus, the elevated temperature alone did not account entirely for the increased diffusion and device degradation. It was the presence of the disordered fused interface (both a source and sink for defects, such as impurities and vacancies) which greatly enhanced diffusion under elevated temperature.

In the fused samples described in this chapter, it is likely that defects (such as vacancies) or impurities (such as hydrogen) were present at the fused interface, and diffused from the fused interface into the surrounding materials, most critically into the base. For instance, hydrogen was certainly present at the fused interface (Figure 4.3). Hydrogen may have diffused into the base and passivated some of the C base doping, hence increasing the base resistance and causing the additional series resistance observed in the diode characteristics of Figures 4.4.b and 4.4.c. (Presently, a series of similar samples are being prepared by S. Estrada and K. McGroddy for base resistance studies.) Figure 4.4.b shows a subset of the data that suggests that reduced fusion temperatures (550-700°C) successfully mitigate the additional series resistance. A similar study is described in Chapter 6, where the electrical performance of as-grown n-AlGaAs/p-GaAs/n-GaAs HBTs is compared to that of

identical HBT structures that have been annealed or formed via fusion of the n-AlGaAs/p-GaAs emitter-base to the n-GaAs collector.

4.5. Wafer-fused Base-Collector Diode Characteristics

Figure 4.4.a shows the I-V curves of base-collector diodes in HBTs formed via fusion over a wide temperature range (550-750°C). (These measurements were taken with the emitter open.) The base-collector leakage current increased with elevated fusion temperature, ranging (at $V_{CB}=25V$) from $2 \times 10^{-6}mA$ for $T_f=550^\circ C$, to 5-10mA for $T_f=700-750^\circ C$. The data of Sections 6.5 and 6.6 (comparing GaAs-GaAs and GaAs-GaN fused interfaces) suggest that this excessive leakage is not inherent to the fusion process (even at as high a temperature as $750^\circ C$). The observed leakage may be due to the GaN material quality, and it may be similar to the emitter-collector leakage prevalent in (Al)GaN HBTs.[11] However, it remains unclear why the leakage would increase with increasing fusion temperature.

The ideality factor (n) also increased with increasing fusion temperature T_f , from $n=2.3-2.9$ at $T_f=550-700^\circ C$, to $n=5.9$ at $T_f=750^\circ C$. It may appear that the wafer fusion process inherently produces a high value of n ; however, it is important to note that epitaxially grown GaN p-n junctions were also reported with high ideality factors ($n \sim 1.5-9.0$).[29, 30] Additionally, Section 6.5 reports that as-grown and fused GaAs-GaAs base-collector junctions demonstrated lower and more uniform ideality factors (1.1-1.5).

It was important to recognize that this base-collector p-n diode structure (formed as part of a tri-layer HBT shown in Figure 4.1) exhibited the opposite trends of the simple (bi-layer) p-n diode structure (Figure 3.1.b). When the simple diodes were fused without the presence of an AlGaAs emitter (Figure 3.4), the ideality factors and reverse-bias leakage currents were observed to decrease with increasing fusion temperature. But for the HBT diodes (Figure 4.4.a), the ideality factors and reverse-bias leakage currents increased with increasing fusion temperature. Not only were the trends reversed, but the ideality factors for the HBT diodes were much worse than for the simple diodes. For HBT diodes formed via fusion for 1 hour, $n=2.3-2.9$ for $T_f=550-700^\circ\text{C}$ and $n=5.9$ for $T_f=750^\circ\text{C}$. For simple diodes also formed via fusion for 1 hour, $n=1.7$ for $T_f=650^\circ\text{C}$, $n=1.5$ for $T_f=700^\circ\text{C}$, and $n=1.4$ for $T_f=750^\circ\text{C}$.

The reason for these discrepancies was difficult to ascertain exactly, but it almost certainly involved diffusion. For example, the gettering properties of the additional (emitter-base) interface may have increased diffusion from the fused base-collector junction toward the emitter-base junction. Although the emitter-base diode characteristics of as-grown and fused samples are nearly identical (as discussed in Section 4.4), there still may have been increased diffusion nearer to the fused interface, thereby affecting the diode characteristics of the fused base-collector junction. Additionally, it may be that defect-assisted diffusion (toward or away from the fused interface) was more prevalent in the thin p-GaAs base (0.15 μm) in the HBT structure, as compared to the thick p-GaAs layer (1 μm) in the diode structure.

Any diffusion effects were likely to increase with increasing fusion temperature, perhaps explaining the increased ideality factors and reverse-bias leakage currents for the base-collector junction in the HBT structure. In contrast, the simple p-n junctions described in Chapter 3 were not adjacent to emitter-base junctions and were not limited to thin p-GaAs layers; without the increased likelihood of defect-assisted diffusion, the electrical performance may have been able to improve with increasing fusion temperature, due to the decreased disorder at the junction induced by higher fusion temperatures (Figure 2.7.b).

4.6. Transistor Characteristics

Gummel plots (Figure 4.5) and common-emitter characteristics (Figure 4.6) were measured for HBTs fused at 50° intervals between 550 and 750°C. Gummel plots indicated that the base current (I_B) was reasonably high for fusion temperatures (T_f) of 550-700°C ($I_B=10-15\text{mA}$ at $V_{BE}=2\text{V}$), but I_B was much lower for the highest T_f of 750°C ($I_B=4\text{mA}$ at $V_{BE}=2\text{V}$). This reduction in base current was to be expected, given the emitter-base degradation in the HBT fused at 750°C (Figures 4.4.b and 4.4.c). Common-emitter I-V curves were dominated by base-collector leakage for HBTs fused at 700-750°C, but were well-behaved for the lower T_f of 550-650°C. The d.c. common-emitter current gain (β) increased with increasing T_f , but consistently remained low. Current gain increased from $\beta=0.29$ for $T_f=550^\circ\text{C}$, to $\beta=1.2$ for $T_f=600^\circ\text{C}$. β was undetermined for HBTs fused at 700-750°C, as these

devices were dominated by base-collector leakage. It was important to recognize that the observed collector currents were not due to emitter-collector leakage currents,[12] which remained at least an order of magnitude lower than the base and collector currents in the range of high enough voltage ($V \sim V_{E-B \text{ turn-on}}$). It was interesting to note that the emitter-collector leakage current increased with increasing T_f , as did the base-collector leakage current.

Mid-range fusion temperatures (600-650°C) produced the most optimal device performance. Poor performance resulting from a low fusion temperature may have been due to the increased disorder observed at interfaces that have been formed via fusion at insufficiently high temperatures (Figure 2.7). Poor performance resulting from a high fusion temperature was more difficult to explain. It was noted in Section 4.5 that the base-collector leakage current increased with increasing fusion temperature. It was further noted that the likely reason was an increase in defect-assisted diffusion with the increased fusion temperatures. SIMS data (Figures 4.2 and 4.3) verified the occurrence of diffusion, and indicated large concentrations of all species (H, O, C, Si) at the fused interface. However, even with complete and accurate information regarding the chemical composition of the fused interface, it was unknown (from the SIMS data alone) whether the various species were behaving in p-type, n-type, or insulating manners. As discussed in Section 2.3, it would have been interesting to assess if and how ΔE_C varied with the many fusion conditions and the many base-collector material designs studied throughout the course of this dissertation work.

The common-emitter current gain (β) was consistently low, and it was important to understand the major limitations of β . Under the conditions that the emitter injection coefficient was nearly ideal (~ 1), β would have the following dependence: [25]

$$\beta = 2 D_{nB} \tau_{nB} / W_B^2$$

where:

D_{nB} = minority carrier (electron) diffusivity in the base

τ_{nB} = minority carrier (electron) lifetime in the base

W_B = width of the base (0.15 μm)

Since the emitter-base junction was an MBE-grown AlGaAs-GaAs heterostructure, one might have expected this AlGaAs-GaAs-GaN HBT to exhibit values of β comparable to those demonstrated in AlGaAs-GaAs-GaAs HBTs. ($\beta \sim 20$ -100 was reported for similar emitter-base structures and device sizes.[20, 21] Chapter 6 further compares AlGaAs-GaAs-GaN and AlGaAs-GaAs-GaAs HBTs.) However, as discussed in Section 4.4, the base of the fused HBT could have been degraded by the fusion process in a number of ways, perhaps including the diffusion of hydrogen from the fused junction into the base, and the subsequent hydrogen passivation of carbon dopants in the base. Diffusion effects may have reduced both τ_{nB} and D_{nB} , leading to a reduced value of β . Lower temperatures should ideally mitigate such diffusion effects; this was consistent with the improved characteristics observed with HBTs formed via fusion at temperatures lower than 700°C (Figures 4.5 and 4.6) If hydrogen were indeed passivating the carbon base dopant, correspondingly the base

resistance should have increased. Samples are presently being prepared (by S. Estrada and K. McGroddy) for measurement of the p-GaAs base resistance after fusion at various temperatures.

In addition, the ΔE_C of +0.4eV at the fused base-collector junction (estimated in Section 2.3) was likely to induce a collector current blocking effect, hence reducing β . Current blocking was also suggested by the increase of β with increasing V_{CE} (Figure 4.6.a-c). It was widely known that optimization of an HBT material structure can be used to mitigate current blocking effects. One possible solution was the addition of a base-collector setback layer, described in the following chapter.

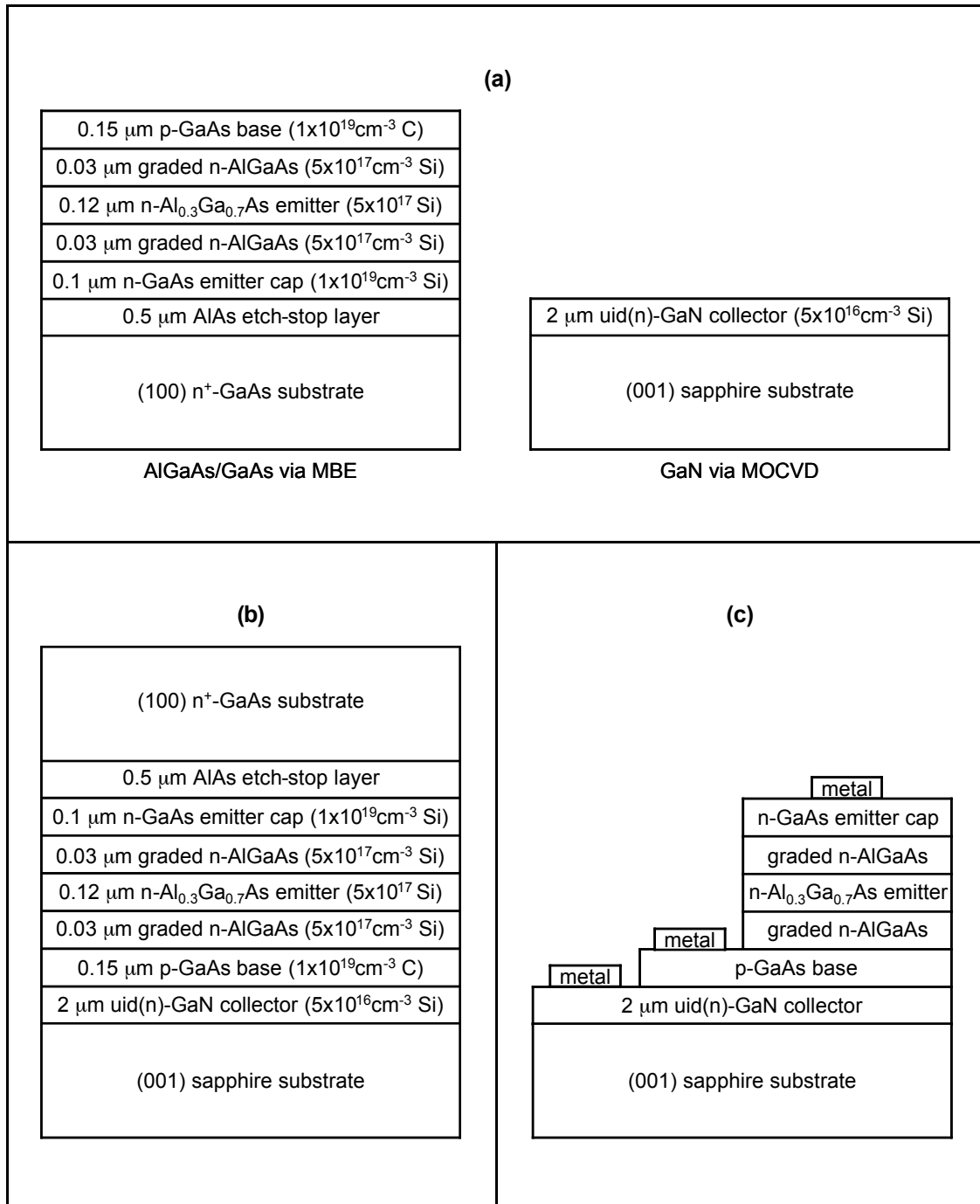


Figure 4.1. The fabrication process for the wafer-fused HBT: (a) starting materials, (b) sample after fusion and before GaAs substrate removal, and (c) I-V test structure after mesa etching and contact metallization.

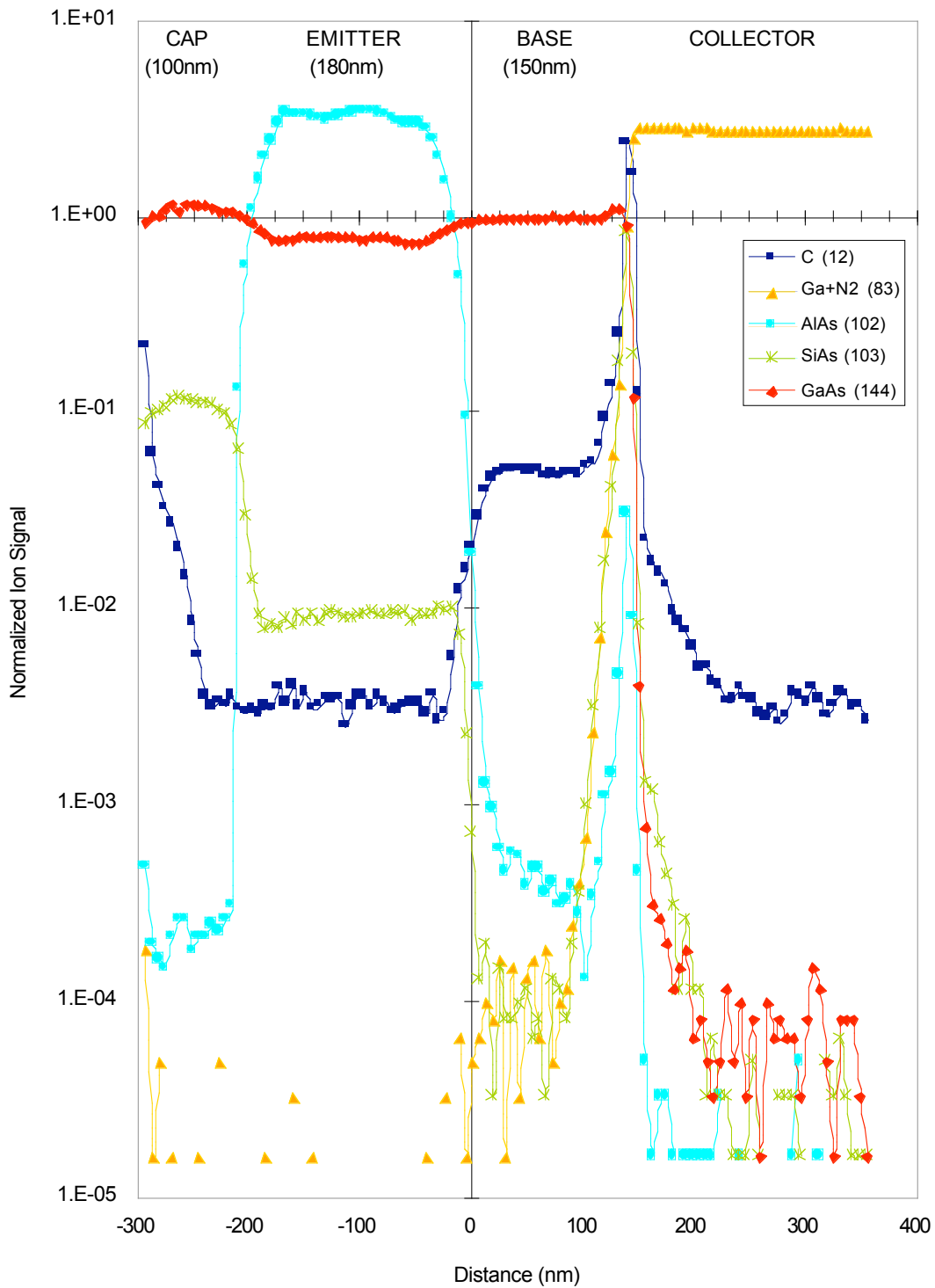


Figure 4.2. Depth profile obtained via secondary ion mass spectrometry (SIMS). This HBT sample was formed via wafer fusion at 600°C for one hour. These SIMS data were obtained in collaboration with Tom Mates at the University of California at Santa Barbara.

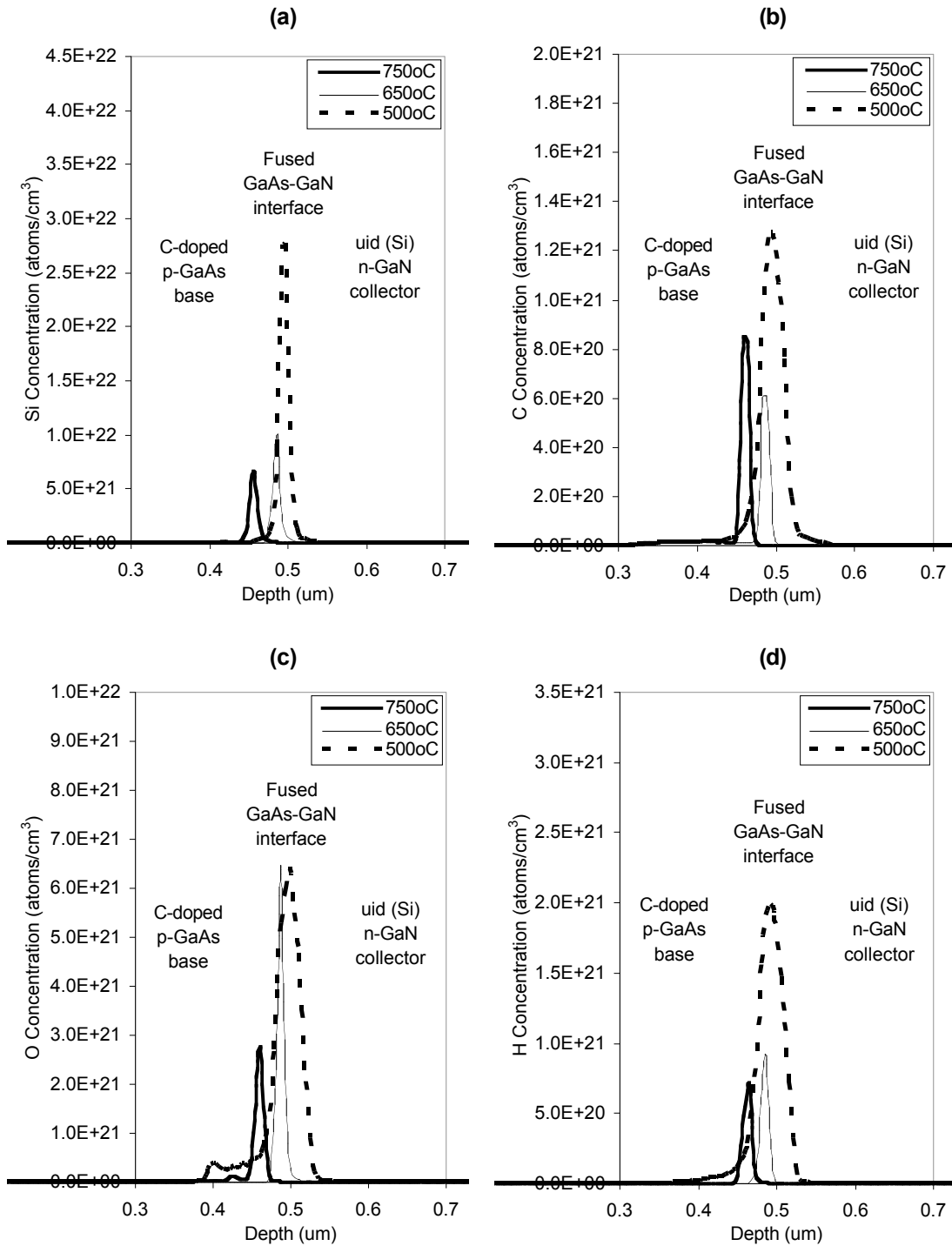


Figure 4.3. SIMS profiles in various samples of the same HBT structure (Figure 4.1.c), all fused for one hour but each fused at a different temperature (500-750°C). Profiles are shown for (a) silicon, (b) carbon, (c) oxygen, and (d) hydrogen. These SIMS data were obtained in collaboration with Yumin Gao at Applied Microanalysis Labs, Inc.

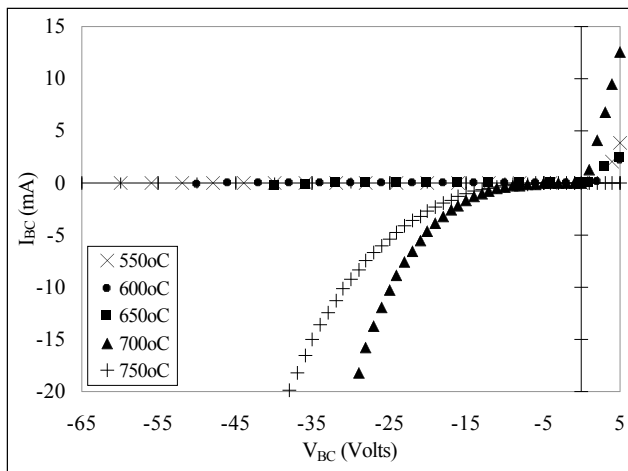


Figure 4.4.a. I-V characteristics (emitter-open) of base-collector diodes in HBT structures formed via wafer fusion at 550-750°C for one hour.

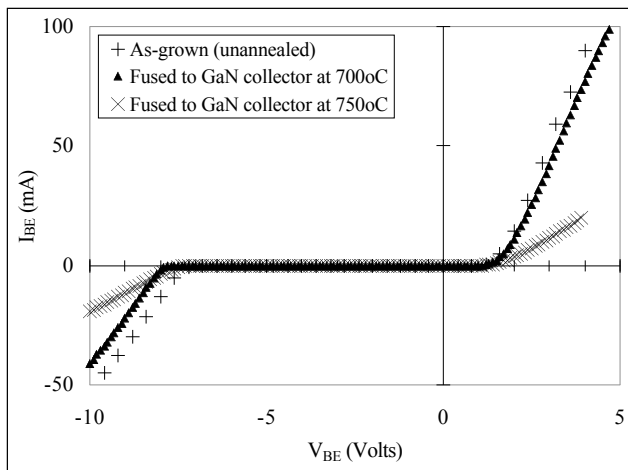


Figure 4.4.b. I-V characteristics of the as-grown emitter-base diode (prior to fusion), and of the base-emitter diodes (collector-open) in HBT structures formed via wafer fusion at 700°C and 750°C for one hour.

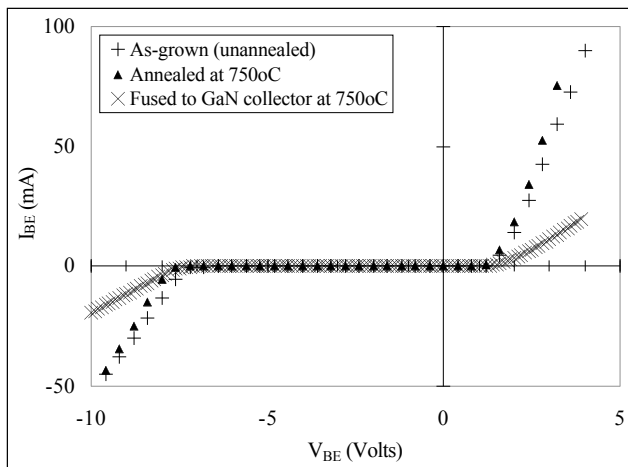


Figure 4.4.c. I-V characteristics of the MBE-grown emitter-base diode subjected to three different thermal processes: as-grown and unannealed, capped and annealed at 750°C for one hour, and wafer-fused to an n-GaN collector at 750°C for one hour.

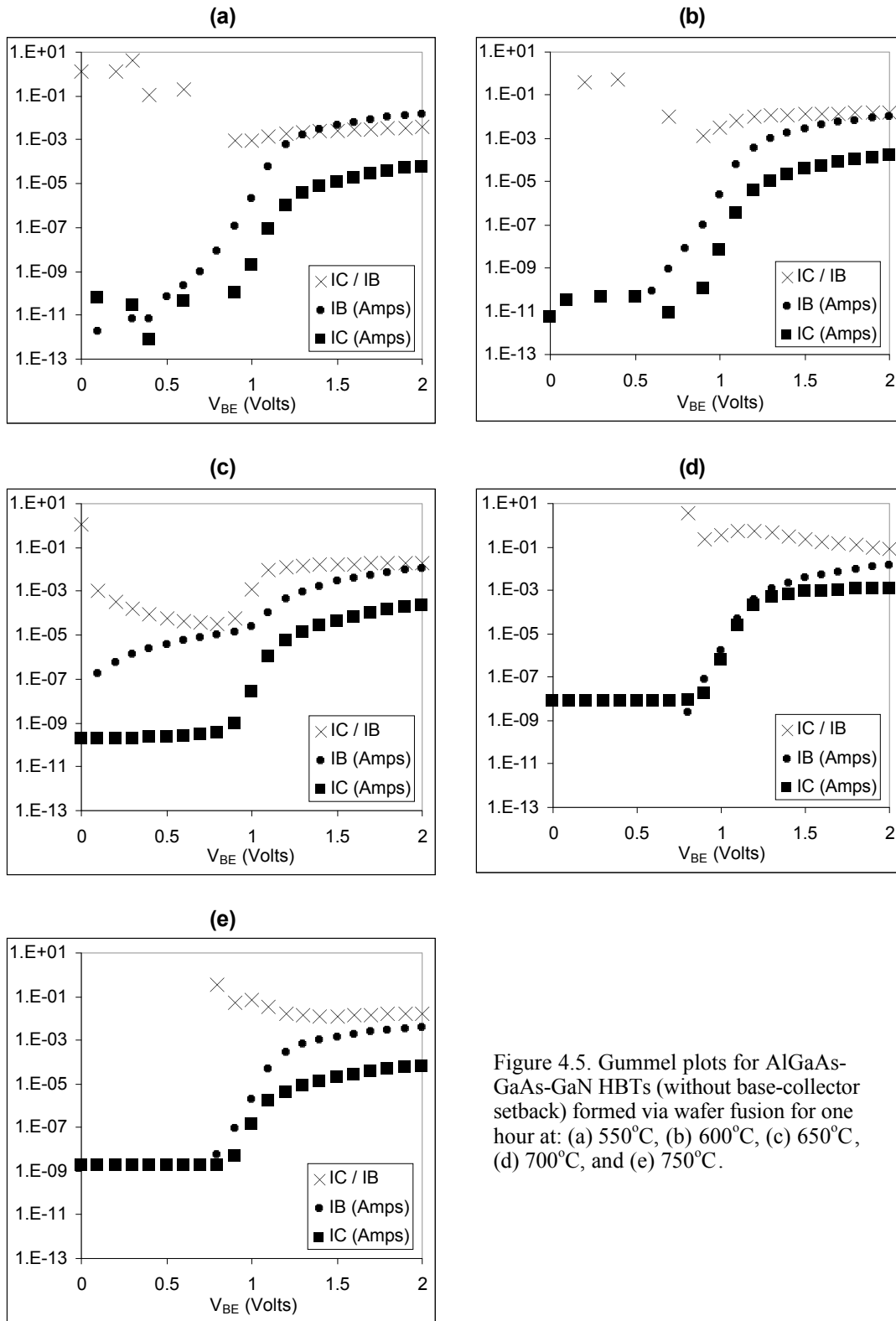


Figure 4.5. Gummel plots for AlGaAs-GaAs-GaN HBTs (without base-collector setback) formed via wafer fusion for one hour at: (a) 550°C, (b) 600°C, (c) 650°C, (d) 700°C, and (e) 750°C.

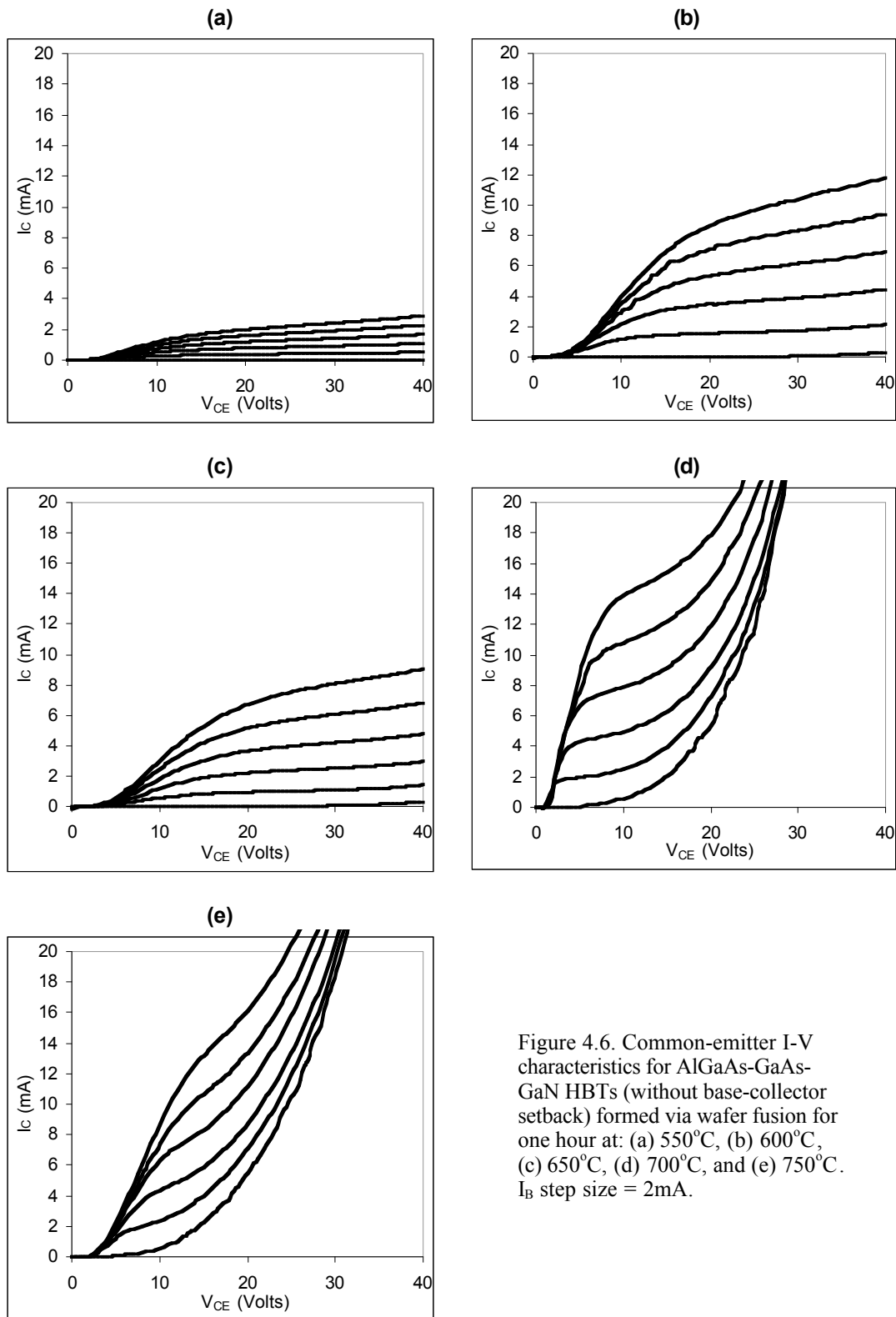


Figure 4.6. Common-emitter I-V characteristics for AlGaAs-GaAs-GaN HBTs (without base-collector setback) formed via wafer fusion for one hour at: (a) 550°C, (b) 600°C, (c) 650°C, (d) 700°C, and (e) 750°C. I_B step size = 2mA.

4.7. References

- [1] X. A. Cao, S. J. Pearton, and F. Ren, "Advanced processing of GaN for electronic devices," *Critical Reviews in Solid State and Materials Sciences*, vol. 25, pp. 279-390, 2000.
- [2] S. Y. Chiu, A. F. M. Anwar, and S. L. Wu, "Base transit time in abrupt GaN/InGaN/GaN and AlGaN/GaN/AlGaN HBTs," *Materials Research Society (MRS) Internet Journal of Nitride Semiconductor Research*, vol. 4, pp. G6.7, 1999.
- [3] T. P. Chow, V. Khemka, J. Fedison, N. Ramungul, K. Matocha, Y. Tang, and R. J. Gutmann, "SiC and GaN bipolar power devices," *Solid-State Electronics*, vol. 44, pp. 277-301, 2000.
- [4] G. Dang, B. Luo, A. P. Zhang, X. A. Cao, F. Ren, S. J. Pearton, H. Cho, W. S. Hobson, J. Lopata, J. M. van Hove, J. J. Klaassen, C. J. Polley, A. M. Wowchack, P. P. Chow, and D. J. King, "npn AlGaN/GaN heterojunction bipolar transistors and GaN bipolar junction transistors with regrown C-doped GaAs in the base regions," *Solid-State Electronics*, vol. 44, pp. 2097-2100, 2000.
- [5] J. Han, A. G. Baca, R. J. Shul, C. G. Willison, L. Zhang, F. Ren, A. P. Zhang, G. T. Dang, S. M. Donovan, X. A. Cao, H. Cho, K. B. Jung, C. R. Abernathy, S. J. Pearton, and R. G. Wilson, "Growth and fabrication of GaN/AlGaN heterojunction bipolar transistor," *Applied Physics Letters*, vol. 74, pp. 2702-2704, 1999.
- [6] K. Kumakura, T. Makimoto, and N. Kobayashi, "Common-emitter current-voltage characteristics of a pnp GaN bipolar junction transistor," *Applied Physics Letters*, vol. 80, pp. 1225-1227, 2002.
- [7] K. P. Lee, A. P. Zhang, G. Dang, F. Ren, J. Han, S. N. G. Chu, W. S. Hobson, J. Lopata, C. R. Abernathy, S. J. Pearton, and J. W. Lee, "Self-aligned process for emitter- and base-regrowth GaNHBTs and BJTs," *Solid-State Electronics*, vol. 45, pp. 243-247, 2001.
- [8] J. B. Limb, H. Xing, B. Moran, L. McCarthy, S. P. DenBaars, and U. K. Mishra, "High voltage operation (> 80 V) of GaN bipolar junction transistors with low leakage," *Applied Physics Letters*, vol. 76, pp. 2457-2459, 2000.

- [9] L. S. McCarthy, P. Kozodoy, M. J. W. Rodwell, S. P. DenBaars, and U. K. Mishra, "AlGaIn GaN heterojunction bipolar transistor," *IEEE Electron Device Letters*, vol. 20, pp. 277-279, 1999.
- [10] J. T. Torvik, M. Leksono, J. I. Pankove, and B. Van Zeghbroeck, "A GaN/4H-SiC heterojunction bipolar transistor with operation up to 300 degrees C," *Materials Research Society (MRS) Internet Journal of Nitride Semiconductor Research*, vol. 4, 1999.
- [11] H. Xing, S. Keller, Y. F. Wu, L. McCarthy, I. P. Smorchkova, D. Buttari, R. Coffie, D. S. Green, G. Parish, S. Heikman, L. Shen, N. Zhang, J. J. Xu, B. P. Keller, S. P. DenBaars, and U. K. Mishra, "Gallium nitride based transistors," *Journal of Physics-Condensed Matter*, vol. 13, pp. 7139-7157, 2001.
- [12] H. Xing, D. Jena, M. J. W. Rodwell, and U. K. Mishra, "Explanation of anomalously high current gain observed in GaN-based bipolar transistors," *IEEE Electron Device Letters*, vol. 24, pp. 4-6, 2003.
- [13] S. Yoshida and J. Suzuki, "High-temperature reliability of GaN electronic devices," *Materials Research Society (MRS) Internet Journal of Nitride Semiconductor Research*, vol. 5, 2000.
- [14] A. P. Zhang, J. Han, F. Ren, K. E. Waldrip, C. R. Abernathy, B. Luo, G. Dang, J. W. Johnson, K. P. Lee, and S. J. Pearton, "GaN bipolar junction transistors with regrown emitters," *Electrochemical and Solid State Letters*, vol. 4, pp. G39-G41, 2001.
- [15] G. W. Neudeck, *The Bipolar Junction Transistor*, vol. 3, 2 ed., Addison-Wesley (Reading, Massachusetts), 1989.
- [16] B. G. Streetman, *Solid State Electronic Devices*, 4th ed., Prentice Hall (Englewood Cliffs, New Jersey), 1995.
- [17] P. M. Asbeck, F. M. C. Chang, K. C. Wang, G. J. Sullivan, and D. T. Cheung, "GaAs-Based Heterojunction Bipolar-Transistors for Very High-Performance Electronic-Circuits," *Proceedings of the IEEE*, vol. 81, pp. 1709-1726, 1993.
- [18] M. G. Chen and J. K. Notthoff, "A 3.3-V 21-Gb/s PRBS generator in AlGaAs/GaAs HBT technology," *IEEE Journal of Solid-State Circuits*, vol. 35, pp. 1266-1270, 2000.

- [19] H. K. Ahn, M. El-Nokali, and D. Y. Han, "An efficient algorithm for optimizing the electrical performance of HBTs," *International Journal of Numerical Modelling-Electronic Networks Devices and Fields*, vol. 16, pp. 353-365, 2003.
- [20] A. C. Han, M. Wojtowicz, T. R. Block, X. Zhang, T. P. Chin, A. Cavus, A. Oki, and D. C. Streit, "Characterization of GaAs/AlGaAs heterojunction bipolar transistor devices using photoreflectance and photoluminescence," *Journal of Applied Physics*, vol. 86, pp. 6160-6163, 1999.
- [21] H. Wang, G. I. Ng, H. Q. Zheng, and P. H. Zhang, "A comprehensive study of AlGaAs/GaAs beryllium- and carbon-doped base heterojunction bipolar transistor structures subjected to rapid thermal processing," *Journal of Applied Physics*, vol. 86, pp. 6468-6473, 1999.
- [22] K. Yamamoto, S. Suzuki, K. Mori, T. Asada, T. Okuda, A. Inoue, T. Miura, K. Chomei, R. Hattori, M. Yamanouchi, and T. Shimura, "A 3.2-V operation single-chip dual-band AlGaAs/GaAs HBT MMIC power amplifier with active feedback circuit technique," *Ieee Journal of Solid-State Circuits*, vol. 35, pp. 1109-1120, 2000.
- [23] W. Zhou, J. J. Liou, and C. I. Huang, "A semi-empirical model for the AlGaAs/GaAs HBT long-term current instability," *Solid-State Electronics*, vol. 44, pp. 541-548, 2000.
- [24] C. R. Abernathy and F. Ren, "Effect of Base Dopant Species on Heterojunction Bipolar-Transistor Reliability," *Materials Science and Engineering B-Solid State Materials for Advanced Technology*, vol. 28, pp. 232-237, 1994.
- [25] W. Liu, *Handbook of III-V Heterojunction Bipolar Transistors*, Wiley (New York, New York), 1998.
- [26] H. Xing, Ph.D. Dissertation: *Growth, fabrication and characterization of gallium nitride based bipolar transistors*, Electrical and Computer Engineering Department, University of California, Santa Barbara, 2003.
- [27] J. Mimila-Arroyo and S. W. Bland, "Hydrogen co-doping in III-V semiconductors: Dopant passivation and carbon reactivation kinetics in C-GaAs," *Modern Physics Letters B*, vol. 15, pp. 585-592, 2001.
- [28] K. A. Black, P. Abraham, A. Karim, J. E. Bowers, and E. L. Hu, "Improved Luminescence from InGaAsP/InP MQW Active Regions using

a Wafer Fused Superlattice Barrier," presented at IEEE 11th International Conference on Indium Phosphide and Related Materials (Davos, Switzerland), pp. 357-360 (TuB4-3), 1999.

- [29] J. B. Fedison, T. P. Chow, H. Lu, and I. B. Bhat, "Electrical characteristics of magnesium-doped gallium nitride junction diodes," *Applied Physics Letters*, vol. 72, pp. 2841-2843, 1998.
- [30] P. Kozodoy, Ph.D. Dissertation: *Magnesium-doped gallium nitride for electronic and optoelectronic device applications*, Electrical and Computer Engineering Department, University of California, Santa Barbara, 1999.